

# 歯科用修復材料の微小表面接触疲労試験における疲労特性

藤井 孝一

鹿児島大学大学院医歯学総合研究科  
先進治療科学専攻 顎顔面機能再建学講座  
歯科生体材料学分野

## Fatigue characteristics of dental restorative materials in a surface-contact fatigue test

Koichi Fujii

Department of Biomaterials Science,  
Field of Oral and Maxillofacial Rehabilitation, Course for Advanced Therapeutic,  
Kagoshima University Graduate School of Medical and Dental Sciences,  
8-35-1 Sakuragaoka, Kagoshima 890-8544, Japan

### Abstract

It is recognized that wear processes of dental restorative materials may be related in part to surface fatigue. One of the major limitations to the use of posterior restorative materials has been localized material loss in contact areas, due to fatigue. Despite this clinical problem it has been difficult to devise a method which is suitable for the study of the surface fatigue of restorative materials *in-vitro*. The purpose of review here was to report a method, a rolling-ball device (RBD), for the study of surface fatigue of restorative materials with the following design criteria: The method should produce loss of material by surface fatigue, not bulk fatigue, and to discuss its application to dental materials using a RBD for producing surface fatigue.

**Key words:** Restorative materials, Surface-contact fatigue, Rolling-ball device (RBD), 3D profile, SEM

### 1. Introduction

In many studies of fatigue testing for dental materials, methods used previously include compressive fatigue<sup>1-3)</sup> and flexural fatigue<sup>3-7)</sup> which involve testing cylindrical or beam specimens of materials to destruction through cyclic

loading. These methods, though providing some useful information about the test materials, suffer some disadvantages. Namely, the bulk failure observed when specimens undergo catastrophic failure may not be related to loss of surface material by “fatigue wear”.

Other approaches have involved the application of multiple compressive forces onto the surfaces of test materials in order to produce surface (as opposed to bulk) degradation<sup>8,9)</sup>. In these experiments the fatigue characteristics were assessed indirectly by observing cracks and damage zones on the sectioned surfaces of the test specimens. A similar method<sup>10)</sup> has been used to induce marginal defects in composites through a fatigue mechanism.

Therefore, a method of producing and evaluating surface fatigue using a rolling-ball device has been developed. The method is based on the principle of “rolling ball” applying cyclic loading onto the surface of a test specimen, and involves constraining a rolling ruby ball between the “V” groove of rotor and the test specimen. Surface failure is detected by the development of a “fatigue track”. In this review, the methods, RBDs were compiled, and the results of its application to dental materials were compared.

## 2. Experimental procedure

### 2-1. Rolling-ball device (RBD)

The rolling-ball surface fatigue device is shown in Fig. 1, designed by McCabe et al.<sup>11,12)</sup>. It consists of a balanced beam which is constructed from a quartz rod pivoted at a frictionless stainless steel hinge. The specimen holder is located at one end of the balanced quartz beam and this is counterbalanced by weights at the other end of the beam. The other main component of the equipment is the electric motor which is used to drive a “V” grooved stainless steel rotor.

The rolling ball is constrained between the “V” groove of the rotor and the test specimen surface resulting in three point contacts (2 contacts with the “V” groove of the rotor and one with the specimen surface). This ensures that the ball rolls and does not slide during testing. The load on the ball during testing was determined by the position of the counterweights on the balanced beam. After setting up the equipment the counter weights were moved to a position such that a predetermined load was transferred to the rotor-ball-specimen assembly. The test load was confirmed using a calibrated load-cell. The speed of rotation of rotor and the ball were determined using two methods. Firstly, a stroboscope was used to determine the rotational speed of the rotor (a dab of white paint was used to facilitate this procedure) and the speed of the rolling ball as it completed a circuit of the “V”-groove rotor and specimen surface.

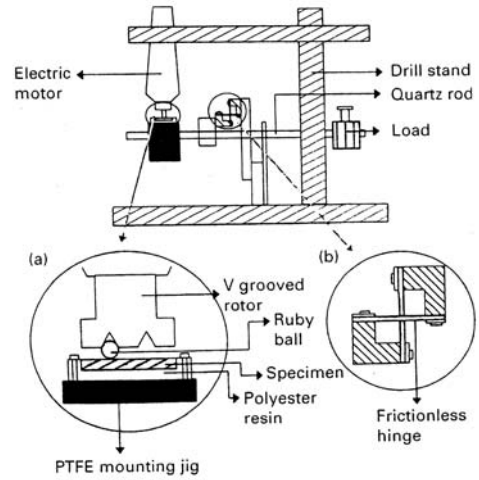


Fig. 1 Line diagram of the rolling ball surface fatigue apparatus.

Secondly, a digital tachometer was used to confirm the speed of rotation of the rotor and to eliminate any harmonic effects of the strobe light.

### 2-1-1. Test procedure

The specimen holders, containing the test specimen, was located at one end of the balanced beam. Its position was fixed through two pins which pass through the holes in the specimen block and into the PTFE mounting jig (Fig 1). The specimen was leveled using a spirit level and the test load (200g) established through altering the position of the counter-weight. A 2 mm diameter ruby ball was located between the test specimen surface and the “V” groove of the rotor. A distilled water drip was used to wet the specimen surface during testing. The rotor was switched on and the rotor and ball set to rotate at a predetermined speed (the ball completes 17 rps).

### 2-1-2. Fatigue track depth determination

At regular intervals during testing the motor was switched off and the specimen removed from the test rig for evaluation. Profilometry was performed in order to determine the depth of any fatigue track which had developed. Having previously determined that the profile results were reproducible at different sectors of the fatigue track, the standard evaluation procedure was to profile each specimen twice at 90 ° and resulted in four equidistant

determinations of fatigue track depth. The profiling instrument had a maximum Z displacement of 200  $\mu\text{m}$  and was accurate to  $-0.1 \mu\text{m}$ . After profiling, the specimen was replaced on to the equipment for further testing. The fatigue life was defined as the time (number of cycles) up to the point where surface degradation occurred. It was not easy to precisely determine this point and so the time to produce a track depth of 5  $\mu\text{m}$  was used in order to compare materials. This point was determined by interpolation.

**2-2. A modified RBD**

Figure 2 shows a modification of rolling-ball test device<sup>13-15</sup>. In the modified instrument loading is performed through a dead weight applied through a pulley as opposed to a beam device which was designed previously by McCabe et al.. The principle of operation is illustrated in Fig. 2. The rotor and specimen holder were maintained in rigid alignment to avoid the introduction of bending or twisting forces. The ball, which was constrained between

the V groove of the rotor and the test material surface, was set to 720 rpm through a motor which was connected to the rotor. The ball resulted in a point contact perpendicular to the surface of the test specimen. Therefore, the load on the ball can be resolved into two directions as, firstly, a normal load and secondly, the tangential force (frictional force) acting to reverse the direction of rolling at the contact point on the sample surface. Finally, the resultant force acting on the specimen surface by the applied load through the ball (Fig. 3) can be realized and this induces elastic or plastic deformations of the specimen surface, which eventually cause failure. It is a key factor of this test that there is no element of sliding friction<sup>13</sup>.

The evaluation of surface contact fatigue was carried out by determining a surface profile on impressions of the

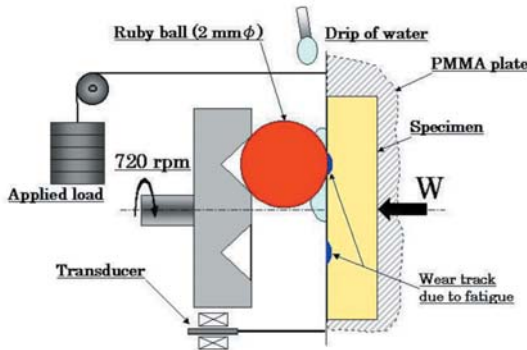


Fig. 2 Schematic representation of RBD apparatus. The contact load W is equivalent to the applied load.

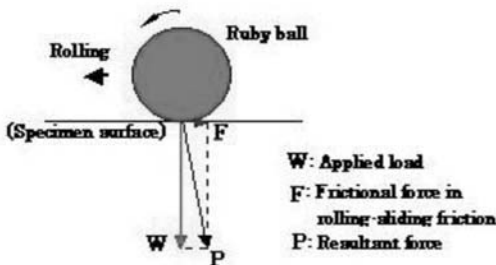


Fig. 3 Schematic representation of composition of forces between rolling-ball and specimen surface.

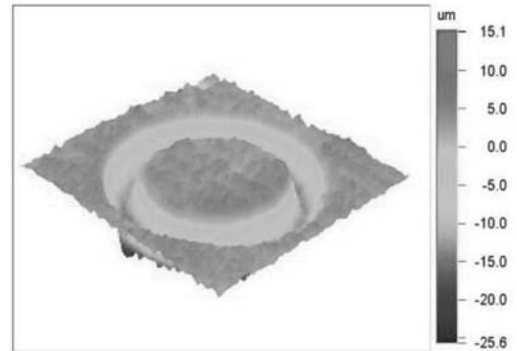


Fig. 4 A typical 3D profile of a fatigue track.

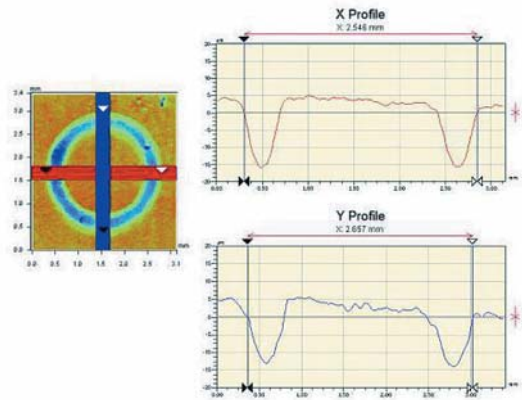


Fig. 5 A typical 2D profile across the surface using cursor widening.

surface of the specimen recorded at regular intervals during testing, using a non-contacting laser profiler. Scanning, in current study was performed as 20  $\mu\text{m}$  intervals on a region 5  $\times$  5  $\text{mm}^2$ , enclosing the impression of the fatigue track circle. The sampling rate during scanning was 500 Hz at a scanning speed of 10 mm/s. A 3 D image of the wear track circle was viewed (Fig.4) and measurements of track depth were made by laying down a measuring cursor across the image and then viewing and measuring on a 2 D profile (Fig. 5). Wear track depth was determined to a precision of 0.5  $\mu\text{m}$  at 90 ° to the plane of the surface of the specimen and was averaged across a 350  $\mu\text{m}$  width using software cursor widening capabilities. The wear track depth was calculated as the mean depth from four such profiles at regular intervals on each of three test specimens and the fatigue life was defined as the number of cycles to produce a track 5  $\mu\text{m}$  deep as determined by interpolation as previously described<sup>(11,12)</sup>.

### 3. Its application of RBD to dental materials

#### 3-1-1. Surface contact fatigue and flexural fatigue of dental restorative materials

Antagonistic contact on a dental restoration may produce surface and subsurface stresses leading to fatigue wear as well as to bulk stressing, eventually causing catastrophic failure. McCabe et al. studied the outcome of two different approaches to fatigue testing of materials involving either surface contact fatigue or flexural fatigue mechanisms<sup>(13)</sup>, and came to the following finding. A range of materials was tested, including conventional glass-ionomers, resin-modified glass ionomers, poly-acid modified composites, and composites. Materials were prepared and tested using both surface contact and flexural fatigue. The results show that conventional glass-ionomers have the least resistance to fatigue under both regimes while composites have the longest fatigue lives and the highest values of flexural fatigue limit (Tables 1 & 2). Microfilled composite are noticeably more resistant to surface contact fatigue than hybrid type composites despite the fact that the bulk flexural fatigue behavior of these two groups of materials suggests opposite ranking. It is considered that these results were influenced not only by the ultimate strength of each material, but also the elastic modulus, toughness and viscoelasticity<sup>(13)</sup>. This complex basis for the explanation of contact fatigue is further

**Table 1 Surface contact fatigue life**

Material	Number of cycles to failure	
	Mean* $\times 10^3$	SD $\times 10^3$
Shofu FX	1.44 <sup>a</sup>	0.19
Shofu Type	1.63 <sup>a</sup>	0.72
Vitmer	9.15 <sup>b</sup>	0.91
Dyract	51.8 <sup>c</sup>	5.35
Silux Plus	1339	200
Z100	42.7 <sup>c</sup>	18.1

\*Means with same letter attached are not significantly different,  $p > 0.05$ .

**Table 2 Flexural fatigue limit**

Material	Fatigue limit at $10^4$ flexural cycles (MPa)	
	Mean*	SD
Shofu FX	28.8 <sup>a</sup>	4.6
Shofu Type	26.9 <sup>a</sup>	1.6
Vitmer	53.0 <sup>b</sup>	10.2
Dyract	72.9 <sup>c</sup>	14.7
Silux Plus	72.5 <sup>c</sup>	3.4
Z100	126.3 <sup>d</sup>	3.1

\*Means with same letter attached are not significantly different,  $p > 0.05$ .

supported by the evidence that optimum resistance to contact fatigue for resin matrix composites occurs at intermediate levels of filler loading indicating that simple properties like hardness and stiffness cannot be directly correlated with contact fatigue<sup>(11)</sup>. The lower modulus, microfilled product has an ability to support compressive loading beneath a sphere without developing subsurface stresses of magnitude great enough to cause rapid crack propagation, which would be manifested as wear. These findings are in agreement with clinical findings that suggest that microfilled products often have wear resistance superior to hybrid products in occlusal contact areas, but the same materials are more likely to suffer catastrophic fracture<sup>(16)</sup>. However, the results also support the fact that catastrophic failure should be investigated separately from surface contact fatigue.

#### 3-1-2. Surface contact fatigue life with series of model dental composites

McCabe et al. suggested that a method of producing and evaluating surface fatigue using a RBD is simple and

reproducible and allows fatigue data to be gathered using a relatively small number of specimens. They investigated a series of model dental composites having varying filler fractions (23.7-66.4 vol%) in order to assess the potential of the method. The results have been that the pattern of material loss as well as scanning electron microscopy (SEM) examination of the damaged surface of test specimens confirmed that a fatigue mechanism was responsible for material loss (Fig. 6). And the fatigue life varied markedly with filler volume fraction being optimized at values in the range 30-50 vol%, and lower and higher volume fractions reduced the fatigue life (Fig. 7). In addition, the contact

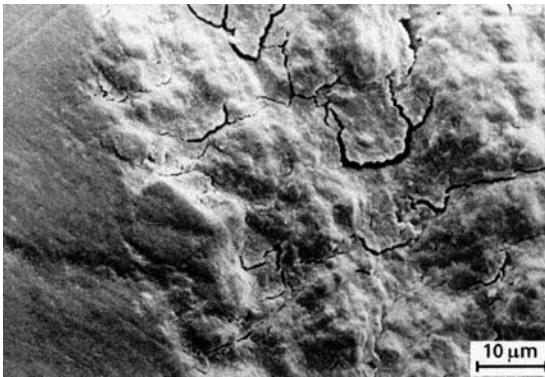


Fig. 6 SEM photomicrograph showing surface of material which has been subjected to rolling ball fatigue. Note the loss of materials, the exposure of subsurface cracks and the lack of scratches due to sliding.

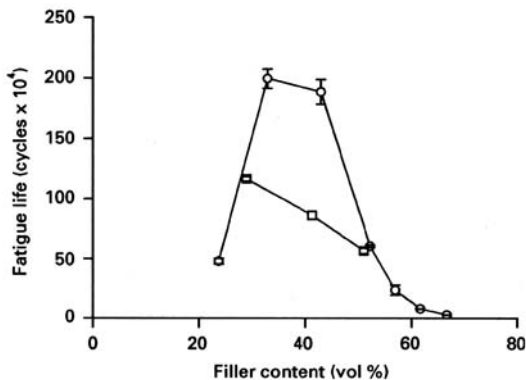


Fig. 7 Fatigue life (number of cycles survived before surface degradation) plotted against filler volume fraction for ; ( ) silanated and ( ) un-silanated glass filler.

fatigue life of a non-silanated composite resin containing 40% filler was approximately 1/2 that of a similar material with silanated filler, and filler silanation significantly improves surface fatigue life. This study did point to the importance of filler silanation as a factor, which helps to optimize contact fatigue life. The results also suggest that the RBD will prove useful in comparing the properties of different materials and in the development of improved products.

### 3-1-3. Effect of the applied load on surface contact fatigue of filling materials using the modified RBD

In order to evaluate material durability, fatigue testing of dental materials has generally been carried out by means of tensile, compressive and flexural testing using constant applied stress or strain to bulk test specimens<sup>1-4</sup>. The mechanism of failure in such tests involves a marked increase in stress in the region of surface or near-surface flaws or imperfections (such as air bubbles) leading to crack growth and fracture at a specific site under repeated loading<sup>2, 4</sup>. In such fatigue tests the final fracture occurs suddenly and immediately prior to fracture there may be no change in the external appearance of the material. Such a mechanism may adequately describe fatigue behavior of materials which results in catastrophic failure but does not adequately describe fatigue which contributes to surface breakdown as part of a surface wear process<sup>6, 17</sup>. Surface degradation within the oral cavity seems to advance due to minute repeated loadings through point or line contacts between pairs materials, e.g. enamel and restorative material<sup>17, 18</sup>. Such a surface contact fatigue wear is unlikely to be predicted from the bulk characteristics of a material but is likely to be specifically related to surface characteristics<sup>11</sup>. Surface contact fatigue wear increases the surface roughness, causes loss of gloss, may cause discoloration and produces deterioration in the esthetics of the material<sup>17</sup>. Moreover, excessive fatigue wear may contribute to functional problems with occluding teeth. Therefore, although the fatigue behavior of a material obtained by testing bulk specimens is important, it is clear that surface contact fatigue characteristics are equally important in estimating the endurance limits of dental filling materials.

As stated previously in chapter 3-1-1, in view of the complex nature of the contact fatigue process and the

inability to relate fatigue life to basic mechanical properties of materials, it is essential to understand the way in which measured fatigue parameters vary with key test conditions such as applied load. Hence, Fujii et al. have attempted to clarify the applied load dependence of fatigue life for two dental filling materials: a microfilled composite (MF: Filtek™ A110, 3M, USA) and a glass ionomer (GF: Fuji II Capsule, GC, Japan), using the modified RBD<sup>13</sup>. Disk specimens 10 mm diameter by 1.5 mm thick were set into cavities cut in plates of PMMA. After setting, the specimens were ground and polished using wet carborundum paper followed by 1  $\mu\text{m}$  alumina and then stored for 24 h in water at 23  $^{\circ}\text{C}$ . The surface fatigue test carried out using loads ranging from 100 to 500 gf through a ruby ball 2 mm diameter using a modified RBD. The ball was set to rotate at 720 rpm and a surface profile was determined on impressions recorded at regular intervals. Fatigue life was defined as the number of cycles to produce a track 5  $\mu\text{m}$  deep and was determined by interpolation<sup>11,12</sup>.

#### Indentation depth with applied load for MF and GF

Fig. 8 shows the static indentation of the 2 mm ruby-ball into the surface of each material as the applied load was increased from 100 to 500 gf and then reduced again. With a 500 gf applied load, the indentation for MF was 1.4 times greater than that for GF. In this study, the indentation of the test materials by ruby ball seems to be through an elastic deformation up to a load of 500 gf, as shown in Fig. 8. Although the values of indentation for unloading were slightly larger than those for loading, this is

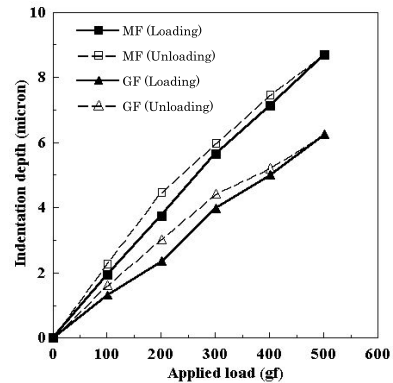


Fig. 8 Variation of indentation depth ( $\mu\text{m}$ ) with applied load for MF and GF specimen.

probably due to a slightly delayed elastic response, although the differences between loading and unloading curves seen in Fig. 8 are so small as to enable the response to be described as “essentially elastic” in nature. The independent-depth might be reduced slightly under conditions of rolling, compared with the static condition, because of slight viscoelasticity which may result in an element of “compressive creep” in the long term. Surface failure in this test is thought to occur through stress concentrations at or near structural defects or inhomogeneities such as porosities, flaws and resin-matrix interfaces occurring within a few microns of surface<sup>19,20</sup>. Thereafter, the degradation of material (fatigue wear) would occur following the propagation of cracks, as the contact area between ruby-ball and specimen surface gradually increases.

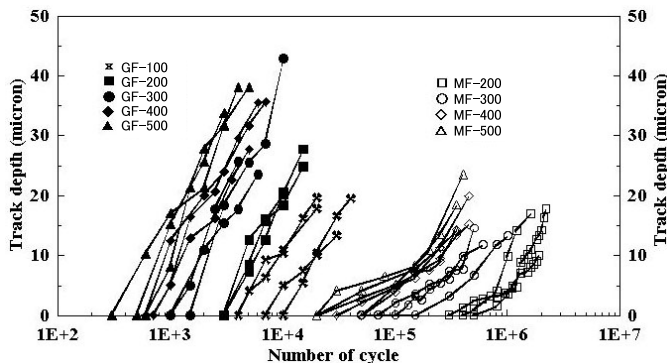


Fig. 9 Variation of track depth ( $\mu\text{m}$ ) with a number of cycles for MF and GF specimens. Load varied from 100 to 500 gf.

**Table 3 Fatigue life (cycles) for MF and GF specimens**

Load (gf)	MF	GF
200	10.6 (1.8) × 10 <sup>5</sup>	4.8 (1.8) × 10 <sup>3</sup>
300	2.8 (1.1) × 10 <sup>5</sup>	1.6 (0.3) × 10 <sup>3</sup>
400	1.2 (0.3) × 10 <sup>5</sup>	0.9 (0.1) × 10 <sup>3</sup>
500	0.7 (0.2) × 10 <sup>5</sup>	0.7 (0.2) × 10 <sup>3</sup>

Values in parentheses are standard deviation (n=3)

**Table 4 Indentation depth and calculated values of stress. Ruby-ball oppressed the specimen surface in a state of rest.**

Material	Load (gf)	Indentation depth (µm)	Stress (MPa)
MF	100	2.1	73.9
MF	500	8.7	90.2
GF	100	1.5	107.2
GF	500	6.2	125.7

**The applied load dependence of fatigue life**

The effect of the applied load on the track depth that is produced by surface contact fatigue is shown in Fig. 9 and Table 3. The number of cycles required for the onset of wear for each material was decreased by increasing the applied load. Clearly, the increase in load causes an increase in stress, which increases the rate of propagation of cracks. In comparing the two test materials, the onset of wear of GF was significantly more rapid than for MF. Furthermore, the rate of material loss for GF, after the start

of the process of surface degradation, as represented in Fig.9, was approximately twice that for MF as shown in the logarithmic plot in Fig. 10. These results are expected from the difference between the indentations measured under static loading as shown in Fig. 8: i.e. the indentation of MF was slightly larger than that of GF, when compared at the same load. This result implies that MF has a greater elastic deformation than GF, and MF is comparatively more flexible and compliant while GF is harder and more rigid. In addition, the compressive strength of a glass ionomer cement is normally lower than that of the yield stress of a microfilled composite resin<sup>21, 22</sup>, and as shown in Table 4 the compressive stresses developed in GF (at 100 and 500 gf), which were calculated from their indentation depth, were close to the compressive strength. Therefore, it seems that the track develops more rapidly for GF partly because it is weaker, harder and more brittle than MF. There was a meaningful positive correlation (R<sup>2</sup> = 0.991 for MF and GF) between incline (rate of loss after initial failure) and load, as shown in Fig. 10 and this can be used alongside fatigue life to characterize the fatigue behavior of the materials.

Table 3 clearly confirms the difference in fatigue life of the two materials used in this study. This result can be partly explained by differences in the basic mechanical properties of the two materials, as already described. However, previous work suggests that this relationship may not survive intact when a broader range of materials is

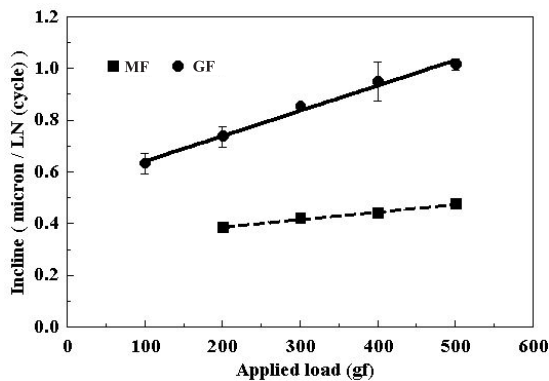


**Fig. 10** Variation of incline of track depth-number of cycles curve with the applied load for MF and GF specimens. The incline was calculated in the range 0-5 µm track.

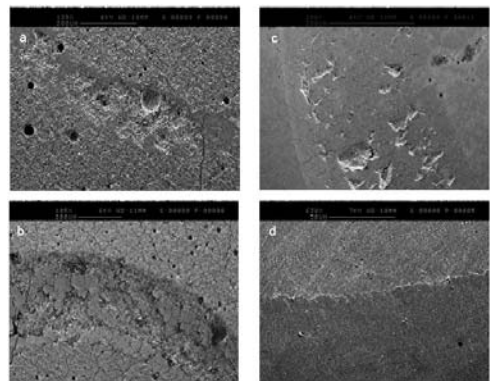


**Fig. 11** SEM photographs for MF and GF specimens. (a) GF, 100 gf, 10 k cycles; (b) GF, 500gf, 700 cycles; (c) MF, 200 gf, 1000 k cycles; (d) MF, 500 gf, 3 k cycles.

considered. Other factors, in particular the presence and location of flaws at or near the surface is likely to be another key factor, and a principal difference between the materials was the existence and distribution of bubbles which were more frequently encountered in GF than in MF, as shown in Fig. 11. In addition to this, another potentially important factor is the greater sensitivity to water of the glass ionomer<sup>17)</sup>. The existence of air bubbles is likely to have a marked effect on both the inherent resistance to contact fatigue and its dependence on applied load, particularly for a hard brittle material.

The variation of Ra and Rt with the applied load

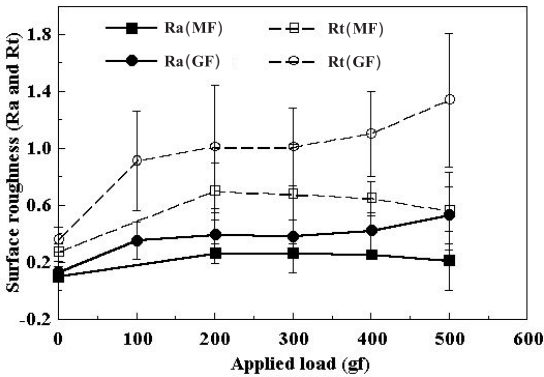


Fig. 12 Variation of mean surface roughness (Ra and Rt) with the applied load for MF and GF specimens. Ra and Rt were average value at each applied load.

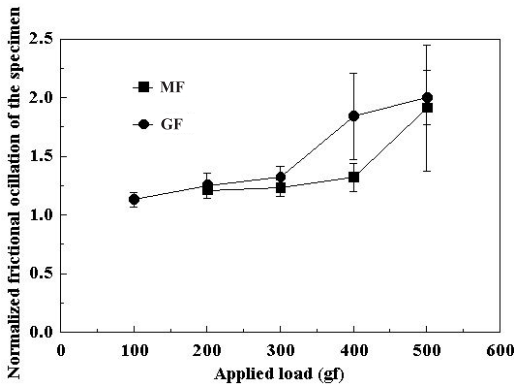


Fig. 13 Variation of normalized frictional oscillation with the applied load for MF and GF specimens.

(Fig.12) might also offer important information which helps to explain the difference in fatigue wear behavior of the two materials. When the applied load increases, the stress increases and this effect will be magnified by an increased surface roughness leading to stress concentration. Furthermore, as degradation begins to occur, roughness increases further and stress is also likely to increase again in response to this. Hence the greater difference in roughness between GF and MF with increasing loading. These results are probably related to the greater brittleness of GF compared with FA. This explanation is also supported by the fact that both the magnitude and variation (scatter) of the frictional oscillation during the rolling of the ruby-ball increased with increasing load, as shown in Fig. 13. The difference in oscillation between 200 and 500 gf was significant for both materials ( $p < 0.05$ ).

SEM images of the track surfaces which correspond to a track depth of 5  $\mu\text{m}$  deep are shown in Fig. 11. Air bubbles and a mixture of fatigue and artefactual cracks caused by desiccation, which are difficult to distinguish by SEM, existed for GF ( Fig. 11a). The existence of these defects, combined with the brittle nature of the material is one factor, which is responsible for lowering the fatigue life of GF compared with MF. This finding is in line with the general finding that porosity in glass ionomer cement, which is primarily introduced during mixing, has a major effect on properties<sup>23)</sup>.

**3-1-4. Studies on surface contact fatigue of other dental materials:**

**Composite resins and PMMAs**

Two composite resins and two PMMAs, as listed in Table 5, were investigated in an atmosphere of dripped distilled water at 37 °. The test procedure, including determining fatigue life, is almost the same as stated previously in chapter 3-1-3, except for rolling-ball rotation of 294 rpm. The surface profile was determined directly on the test

**Table 5 Materials used**

Code	Material	Manufacturer	Filler
ES	Estenia® C & B	Kuraray	88.8
SD	Solidex	Shofu	54.7
AC	Acron	GC	-
SU	Sumipex®	Sumitomo Chem.	-



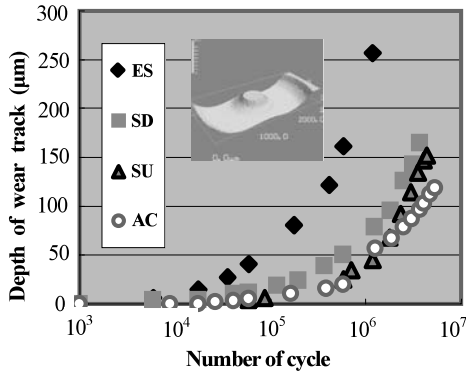


Fig. 14 Variation of depth of wear track (µm) with a number of cycles for four materials.

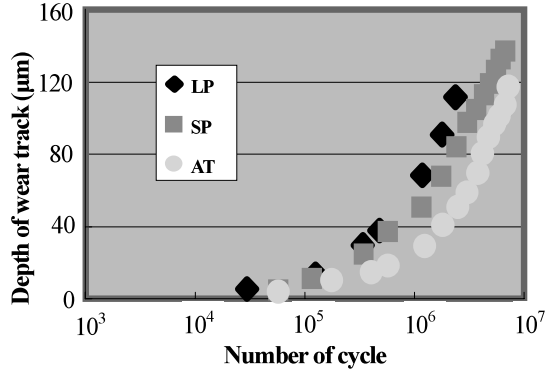


Fig. 16 Variation of depth of wear track (µm) with a number of cycles for three artificial teeth.

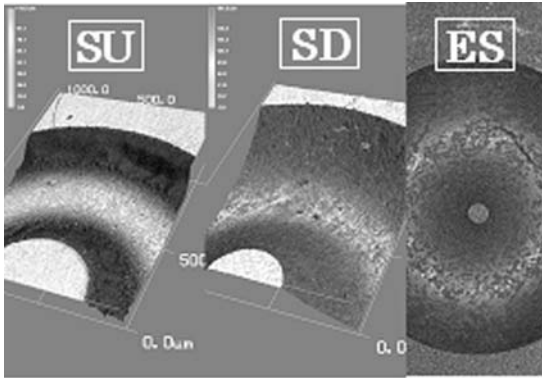


Fig. 15 An expanded view of wear track for three materials. The appearance of wear track with AC is similar to that of SU.

specimen at regular intervals. The fatigue life of four materials was  $5.88 \times 10^3 - 8.82 \times 10^4$  cycles, as shown in Fig. 14. ES containing more inorganic filler (less resin matrix) is not much more resistant to contact fatigue than AC and SU without inorganic filler. For AC and SU without inorganic filler, surface failures like those in ES and SD were never observed after surface-contact fatigue, and their wear track surfaces were comparatively smooth compared with those of ES and SD (Fig. 15). This would be because the resin matrices of AC and SU are a PMMA-based system, and are formed of a homogeneous substance, which is different from the case of composite resin in which several materials having different properties are combined, such as in ES and SD. SU plate is a thermoplastic material, and is

a commercial product of acrylic resin for industrial use; it is free of cross-linking agents and a residual monomer. On the other hand, AC is an acrylic denture-based resin containing a cross-linking agent of approximately 10% EDM A<sup>24</sup>, and is heat-cured using a powder-liquid polymerization method. After polymerization, a residual monomer content of less than 1% usually exists within AC specimen, and this difference of AC and SU might influence the outcome as shown in Fig. 14. At an early stage of surface-contact fatigue, as there have been few cycles, it is considered that the residual monomer near the contact surface might play a role as a plasticizer and hence the fatigue life of AC would be decreased compared with that of SU. However, it can be seen that the effect of the residual monomer on the contact fatigue of AC is less, since the fatigue life of AC is actually reached later than that of SU in current study. Finally, the residual monomer leached out from the contact surface by the dipping water with an increasing number of cycles, and the network structure of resin matrix produced by adding the cross-linking agent has influence upon the increase in fatigue life; hence, the fatigue life of AC might be increased compared with that of SU. However, further detailed studies on the molecular structure and residual are necessary.

**Artificial tooth**

Fig. 16 shows a variation of wear track with a number of cycles for three type artificial teeth (LP: Livdent porcelain; SP: Surpass; AT: Acrylic tooth, All are GC's

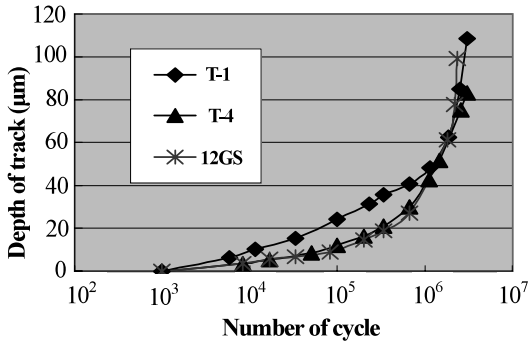


Fig. 17 Variation of depth of wear track (µm) with a number of cycles for three noble metal alloys.

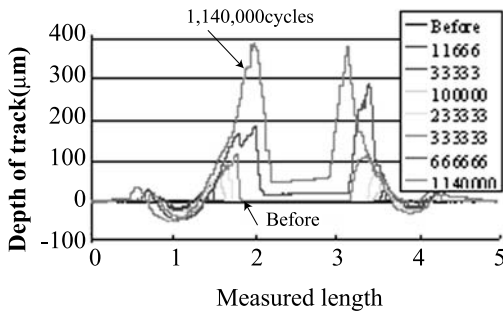


Fig. 18 Variation of depth of wear track (µm) along with a number of cycles for T-1 specimen.

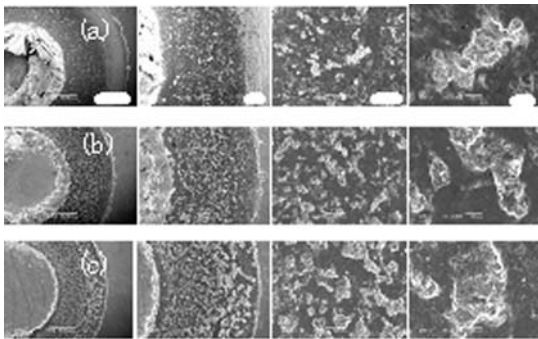


Fig. 19 An expanded view of wear track, The magnification is × 50, × 100, × 200, × 400 from the left: (a) T-1 after  $1.14 \times 10^6$ ; (b) T-4 after  $3.02 \times 10^6$ ; (c) 12GS after  $2.33 \times 10^6$ .

products). The fatigue life of each specimen was ranging from  $3.1 \times 10^4$  -  $5.88 \times 10^4$ , and it was obvious that the greater hardness values of the artificial tooth (Hv, LP: 377; SP: 16.8; AT: 18.6), the deeper wear track depth produced and the more degraded surface of specimen was the same tendency in ES, SD and AC specimens.

**Noble metal alloys**

On the other hand, Figs. 17 and 18 show a variation of depth wear track with a number of cycles for three noble metal alloys in the RBD test. Materials used were Type 1 and 4 gold alloys and 12% gold-silver-palladium alloy of post solution heat treatment at 700 at 30 min.: Their codes are T-1, T-4 and 12GS, respectively, and all are GC’s products. Their fatigue life is ranging from  $10^3$ - $10^4$  (Fig. 17).

Their cross sections of wear tracks were distinctly different from those of the composite resins, acrylic resins and artificial tooth, as described above (Figs. 18 and 19). It seems that the difference is because of expandability of special characteristic of metallic bonding.

**Conclusive remarks**

As described above, the rolling-ball method is able to distinguish the different rates and mechanisms of surface contact fatigue for different materials, and has proved a convenient method for studying the surface fatigue behavior of dental materials. The modified design proved successful in allowing the application of a wide variation of test loads. Although the method differs from those methods which involve testing of the “bulk fatigue” characteristics, the rolling-ball method may give results which are more clinically meaningful. Its use can now be widened to enable comparative testing between different types of materials and studies of the way in which material composition can affect fatigue. Future studies are anticipated.

**Acknowledgment**

The author wishes to thank Professor J F McCabe for many helpful suggestions during the course of this work, and is also grateful to the members of the Department of Biomaterials Science, Graduate School of Medical and Dental Science, Kagoshima University, for their continuing support. This work was supported partly by Grant-in-Aid

for Scientific Research (C) No.19592252, from the Ministry of Education, Culture, Sport, Science and Technology, Japan.

## References

- 1) Draughn, R.A.: Compressive fatigue limits of composite restorative materials. *J Dent Res*, 58, 1094-1096, 1979
- 2) McCabe, J.F., Ogden, A.R.: The relationship between porosity, compressive fatigue limit and wear in composite resin restorative materials. *Dent Mater*, 3, 9-12, 1987
- 3) McCabe, J.F., Carrick, T.E., Chadwick, R.G., Walls, A.W.G.: Alternative approaches to evaluating the fatigue characteristics of materials. *Dent Mater*, 6, 24-28, 1990
- 4) Fujii, K.: Fatigue properties of acrylic denture base resins. *Dent Mater J*, 8, 243-259, 1989
- 5) Asmussen, E., Jørgensen, K.D.: Fatigue strength of some resinous materials. *Scand J Dent Res*, 90, 76-79, 1982
- 6) Drummond, J.L.: Cyclic fatigue of composite restorative materials. *J Oral Rehabil*, 16, 509-520, 1989
- 7) Braem, M.J., Davidson, C.L., Lambrechts, P., Vanherle, G.: In vitro flexural fatigue limits of dental composites. *J Biomed Mater Res*, 28, 1397-1402, 1994.
- 8) Mair, L.H.: Subsurface compression fatigue in seven dental composites. *Dent Mater*, 10, 111-115, 1994
- 9) Htang, A., Ohsawa, M., Matsumoto, H.: Fatigue resistance of composite restorations: Effect of filler content. *Dent Mater*, 11, 7-13, 1995
- 10) Mazer, R.B., Leinfelder, K.F., Russell, C.M.: Degradation of microfilled posterior composite. *Dent Mater*, 8, 185-189, 1992
- 11) McCabe, J.F., Abu Kasim, N.H., Cleary, S.: A rolling-ball device for producing surface fatigue and its application to dental materials. *J Mater Sci*, 32, 283-287, 1997
- 12) McCabe, J.F., Wang, Y., Braem, M.: Surface contact fatigue and flexural fatigue of dental restorative materials. *J Biomed Mater Res*, 50, 375-380, 2000
- 13) Fujii, K., Carrick, T.E., Bicker, R., McCabe, J.F.: Effect of the applied load on surface contact fatigue of dental filling materials. *Dent Mater*, 20, 931-938, 2004
- 14) Fujii, K., Minami, H., Arikawa, H., Kanie, T., Ban, S.: A method for estimation of surface contact fatigue of dental materials. *J J Dent Mater*, 28, 59, 2009
- 15) Fujii, K., Tsuruki, J., Minami, H., Arikawa, H., Kanie, T., Ban, S.: Observation of contact-fatigue surface of dental noble metal alloys. *J J Dent Mater*, 29, 151, 2010
- 16) Lambrechts, P., Braem, M., Vanherle, G.: Evaluation of clinical performance for posterior composite resins and dentin adhesives. *Oper Dent*, 12, 53-78, 1987
- 17) Braem, M., Lambrechts, P., Van Doren, V., Vanherle, G.: In vivo evaluation of four posterior composites: quantitative wear measurements and clinical behavior. *Dent Mater*, 2, 106-113, 1986
- 18) Braem, M., Lambrechts, P., Vanherle, G.: Clinical relevance of laboratory fatigue studies. *J Dent*, 22, 97-102, 1994
- 19) McKinney, J.E., Wu, W.: Relationship between subsurface damage and wear of dental restorative composites. *J Dent Res*, 61, 1083-1088, 1982
- 20) Wu, W., Toth, E.E., Moffa, J.F., Ellison, J.A.: Subsurface damage layer of *in vivo* worn dental composite restoration. *J Dent Res*, 63, 675-680, 1984
- 21) McCabe J.F., Walls, A.W.G.: Applied dental materials. 8<sup>th</sup> ed. McCabe J.F., Walls, A.W.G., eds. 174-182, Blackwell Science, Oxford, 2002
- 22) McCabe J.F., Walls, A.W.G.: Applied dental materials. 8<sup>th</sup> ed. McCabe J.F., Walls, A.W.G., eds. 204-207, Blackwell Science, Oxford, 2002
- 23) Nomoto, R., McCabe, J.F.: Effect of mixing methods on the compressive strength of glass ionomer cement. *J Dent*, 29, 205-210, 2001
- 24) McCabe J.F., Walls, A.W.G.: Applied dental materials. 8<sup>th</sup> ed. McCabe J.F., Walls, A.W.G., eds. 96-99, Blackwell Science, Oxford, 2002